Accurate Ab initio–based force field for predictive CO 2 uptake simulations in MOFs and ZIFs: Development and applications for MTV–MOFs

ARTICLE *in* THE JOURNAL OF PHYSICAL CHEMISTRY C · SEPTEMBER 2012

Impact Factor: 4.77 · DOI: 10.1021/jp307865n

6 AUTHORS, INCLUDING:

Sang Soo Han
Korea Research Institute of Standards and Sci…
58 PUBLICATIONS **1,874** CITATIONS
SEE PROFILE

Daejin Kim
Insilicotech Co.
21 PUBLICATIONS **240** CITATIONS
SEE PROFILE

Sangyeon Cho
Korea Advanced Institute of Science and Tech…
4 PUBLICATIONS **103** CITATIONS
SEE PROFILE

Seung-Hoon Choi
Insilicotech Co.
40 PUBLICATIONS **671** CITATIONS
SEE PROFILE

THE JOURNAL OF PHYSICAL CHEMISTRY C

Article

pubs.acs.org/JPCC

Accurate Ab Initio-Based Force Field for Predictive CO_2 Uptake Simulations in MOFs and ZIFs: Development and Applications for MTV-MOFs

Sang Soo Han,*[,†] Daejin Kim,[‡] Dong Hyun Jung,[‡] Sangyeon Cho,[§] Seung-Hoon Choi,[‡] and Yousung Jung*[,§]

[†]Center for Nanocharacterization, Korea Research Institute of Standards and Science (KRISS), 267 Gajeong-Ro, Yuseong-Gu, Daejeon 305-340, Republic of Korea

[‡]Insilicotech Company Limited, C-602 Korea Bio Park, 210 Sampyong-Dong, Bundang-Gu, Seongnam, Gyeonggi-Do 463-400, Republic of Korea

[§]Graduate School of EEWS, Korea Advanced Institute of Science and Technology (KAIST), Daejeon 305-701, Republic of Korea

Supporting Information

ABSTRACT: For a reliable prediction of CO_2 loading in metal−organic (MOFs) and zeolitic-imidazolate frameworks (ZIFs) by molecular simulation, accurate description of the van der Waals (vdW) and Coulomb interactions is undoubtedly the most critical component. However, there have been some strong recent indications that the use of generic force fields (FFs) widely used in most current CO_2/MOF simulations that were not particularly parametrized for CO_2/MOF and ZIF systems could lead to serious discrepancies compared to experimental results. Here, we develop accurate vdW FFs for CO_2 uptake simulations in MOFs and ZIFs using high-level ab initio calculations, and validate the method by comparing the simulated and experimental CO_2 uptakes for various known MOFs and ZIFs. The agreements between simulations and experiments are shown to be excellent for several known MOFs and ZIFs, although the FF parameters are not specifically fitted to those particular systems, showing the potential transferability of the FF. Atomic charges of the adsorbents are computed via the rapid charge equilibration method. Using these highly accurate FFs, we reveal the origin of the enhanced CO_2 uptake in recently reported MOFs having multivariate functional groups (MTV-MOFs). We find that the capacity enhancement in MTV-MOFs arises from an increase in both vdW (due to tighter geometry) and electrostatic (due to increased dipole moment) interactions between CO_2 and MTV-MOF. We further predict that MOF-5-NO_2 can have an even higher CO_2 uptake than these MTV-MOFs due to a larger local dipole moment of the NO_2-functionalized linker than those found in the reported MTV-MOFs. As a further designing of the high capacity material, we then introduced both electron-donating and -withdrawing functional groups simultaneously in the same organic linker to increase the local dipole moment of the linker significantly. The resulting CO_2 uptake indeed increases substantially due to the favorable electrostatic interactions that can be tested experimentally.

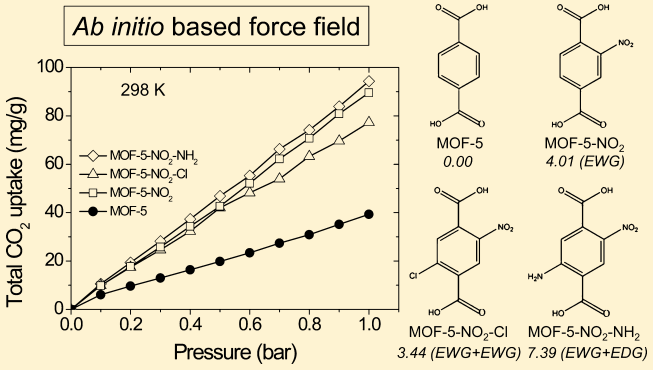

1. INTRODUCTION

Microporous crystalline metal−organic frameworks (MOFs)[1,2] and zeolitic imidazolate frameworks (ZIFs),[3,4] composed of metallic joints (e.g., $Zn_4O(CO_2)_6$ for MOFs and Zn(II) or Co(II) for ZIFs) and organic struts (e.g., 1,4-benzenedicarboxylate for MOFs and imidazolate for ZIFs), represent exceptional porosity (up to 90%) and a high surface area (up to 10 000 m^2/g). These unusual properties of MOFs and ZIFs recently motivated many studies[5−7] to investigate the utility of these materials as a CO_2 adsorbent. MOFs and ZIFs are regarded as one of the more promising CO_2 capture materials today.

One of the key advantages of MOFs or ZIFs is that the porosity, shape, dimension, and surface functionality of these porous materials can be tuned to enhance the CO_2 capacity by systematically changing the combination of inorganic joints and organic struts. This combinatorial library type of screening of MOFs and ZIFs using various known and unknown building blocks is the area where molecular simulations can play a critical and practically very useful role. For example, Yazaydin et al.[8] investigated a diverse set of 14 MOFs for low-pressure CO_2 uptake by atomistic simulations together with experiments, and found that the CO_2 uptake below 1 bar correlates with the heat of adsorption. Similar molecular simulations were also

Received: August 8, 2012
Revised: August 27, 2012
Published: September 5, 2012

performed for several MOF[9] and ZIF[10−13] systems. Recently, predicted by molecular simulations prior to experiments, Farha et al.[2] successfully synthesized an MOF with high surface area, known as NU-100. This NU-100 shows a CO_2 uptake of 2100 mg/g at 298 K.

Usually, the molecular simulation for predicting CO_2 loading in MOFs or ZIFs uses empirical force fields (FFs) to describe van der Waals (vdW) interactions between the adsorbate (CO_2)−adsorbent (MOF or ZIF) and adsorbate−adsorbate, together with Coulomb interactions, by assigning point charges for each atom in the system. Zheng et al.[14] investigated the influence of framework charges on the CO_2 uptake in MOFs and demonstrated that the framework charge contribution in MOFs cannot be ignored in computational screening of MOF materials for CO_2 capture. Currently, several strategies for calculating atomic charges of the MOFs are available. In particular, Wilmer and Snurr[15] reported that the charge equilibration method (Qeq)[16] yielded the similar atomic charges to those of DFT calculations in selected MOFs, although the Qeq calculation is significantly faster than the DFT calculation. Very recently, Haldoupis et al.[17] used the modified Qeq (PQeq) for assigning atomic charges in the periodic structures of MOFs and found that the PQeq charges adequately describe the electrostatic interactions.

As briefly described above, for a reliable prediction of CO_2 loading in MOFs and ZIFs by molecular simulation, accurate description of the vdW and Coulomb interactions is the most critical component. However, to date, most CO_2 uptake simulations in MOFs and ZIFs have been performed using the empirical FFs for the vdW interactions such as UFF[18] and DREIDING[19] that were developed for generic purposes and not specifically optimized for the MOF- or ZIF-CO_2 systems. There are indeed some strong recent indications[12,20−22] that the use of generic FFs widely used in most current CO_2/MOF simulations that were not particularly parametrized for CO_2/MOF and ZIF systems could lead to serious discrepancies compared to experimental results. This means that the use of these existing potentially inaccurate FFs for even largely unknown systems might yield incorrect predictions. Our previous studies[23−26] show that atomistic simulations with ab initio-based FFs reproduced well the experimental H_2[23−25] and CH_4[26] adsorption isotherms in MOF systems. Because of such an importance of FF for predictive simulations, recently there has been an attempt to develop an FF that is specifically optimized for CO_2 and alkali-, alkali-earth, and transition metal-doped COF systems.[27] However, the agreement between the first-principles and the fitted potential energy curves for Li-CO_2 in this study, for example, were only marginal; both repulsive short-range and attractive long-range behaviors were substantially steeper in the results compared to ab initio, and only the equilibrium position and well depth matched between the FF and the ab initio results. Therefore, presently, there is a significant and urgent need for an accurate FF to describe CO_2/MOF and ZIF systems to explain many intriguing experimental phenomena and make reliable predictions for further developments of the field. It is the contribution of our present work that aims at this important task.

Here, we develop accurate atomic vdW FFs for CO_2−CO_2, CO_2−MOF, and CO_2−ZIF systems using high-level ab initio calculations and validate them by comparing the simulated and experimental CO_2 loading for several known MOFs and ZIFs. As applications of the new ab initio-based FFs, we then suggest a strategy for improving CO_2 uptake that can be tested experimentally, and explain the origin of the enhanced CO_2 uptake in recently reported MOFs having multivariate functional groups (MTV-MOFs).

2. MODELING AND COMPUTATIONAL DETAILS

Detailed description of the FF development is often lacking in the literature, and thus we provide here and in the following section the step-by-step prescription of the development procedure for future reference in developing FFs for other gases and frame structures.

Density functional theory (DFT) methods are well-known to lead to poor descriptions of the London dispersion attractive terms dominating weakly bound vdW molecules. Hence, DFT is not useful for predicting proper interaction energies between CO_2 and MOFs and ZIFs. Therefore, we used CCSD(T)[28] and RIMP2.[29] These calculations were carried out with the Q-Chem[30] program.

To develop the CO_2−CO_2 FFs, we calculated the intermolecular potential energy curves for a CO_2 dimer with two configurations—slipped parallel and T-shaped[31]—based on the CCSD(T) calculations with the aug-cc-pVTZ[32] basis. For the interaction of CO_2 with MOFs and ZIFs, we considered various cluster models, such as C_6H_6 and HBDC (H-terminated 1,4-benzenedicarboxylate). The intermolecular binding energies between CO_2 and these model clusters were calculated using the RIMP2 method with cc-pVQZ. All binding energies were corrected using basis set superposition error (BSSE) by the full counterpoise procedure.[33]

On the basis of the accurate quantum mechanical (QM) energetics, we developed FF parameters for the vdW interactions between CO_2−CO_2 and CO_2−MOF/ZIF with the Morse potential form (eq 1). The Morse function is suggested to be more suitable for studying the gas adsorption in porous frameworks than the Lennard-Jones (LJ-12−6) and exponential-6 (exp-6) forms since the LJ-12−6 and exp-6 have inner walls that are often too stiff, and the region with the true $1/R^6$ character appears at much longer distances than are relevant here.[26]

$$U_{ij}(r_{ij}) = D\left\{\exp\left[\alpha\left(1 - \frac{r_{ij}}{r_O}\right)\right] - 2\cdot\exp\left[\frac{\alpha}{2}\left(1 - \frac{r_{ij}}{r_O}\right)\right]\right\} \quad (1)$$

To determine CO_2 adsorption isotherms in MOFs and ZIFs, we used the grand canonical Monte Carlo (GCMC) simulation with the QM-based FFs developed herein. To obtain an accurate measure of CO_2 loading from 0 to 50 bar at 298 K, we equilibrated the system for 1.5×10^6 MC steps, and calculated the average and standard deviation for 0.5×10^6 MC moves in steps of 5000 after the equilibration. Relative errors are less than 0.4%, and hence the average values are only shown. Atomic charges of the frameworks were determined by the original Qeq[16] charge equilibration method, while those of the CO_2 molecule were obtained from the QM calculations. The GCMC simulations used the periodic boundary conditions with the experimental lattice parameters in which the framework atomic positions were fully optimized with the DREIDING[19] FF at the fixed lattice parameters. The excess CO_2 amount was calculated as the total amount of CO_2 contained in the pores minus the amount of the gas that would be present in the pores in the absence of gas−solid intermolecular forces.[34] The GCMC simulations were performed using the Sorption module of the Cerius2 software.[35]

dx.doi.org/10.1021/jp307865n | J. Phys. Chem. C 2012, 116, 20254−20261

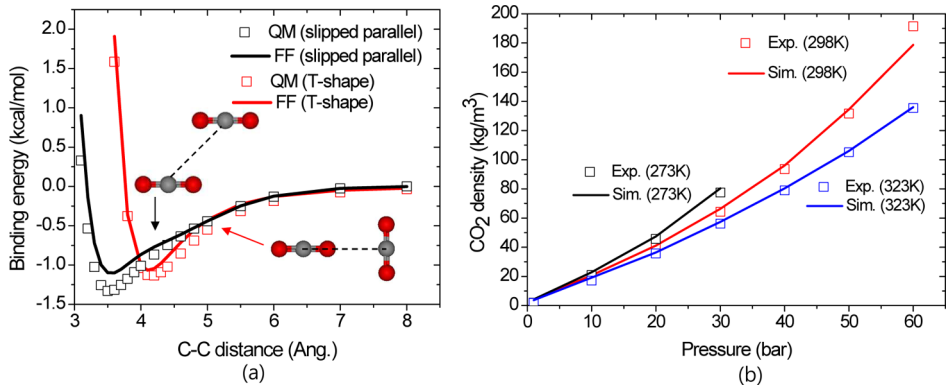

Figure 1. (a) Intermolecular interaction energies (kcal/mol) for a CO_2 dimer calculated at the CCSD(T)/aug-cc-pVTZ level. (b) CO_2 density calculated by a combination of GCMC simulations and the developed FFs at different temperatures (273, 298, and 323 K) as a function of pressure. For comparison, the NIST experimental values[37] are also included.

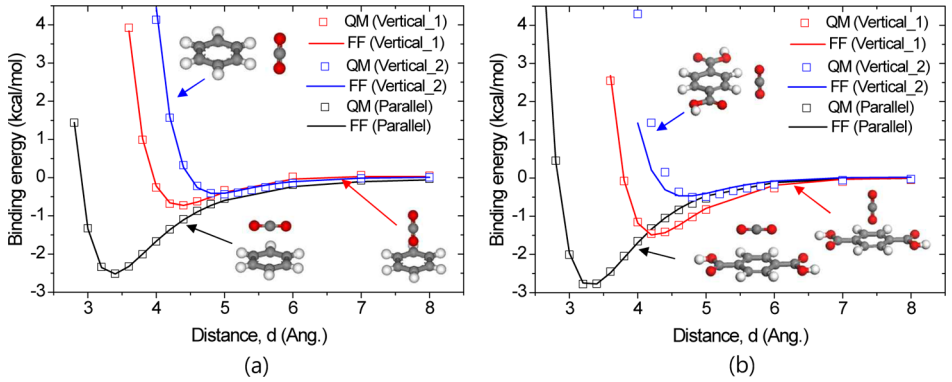

Figure 2. Comparison of the QM (RI-MP2/cc-pVQZ) and fitted (FFs) interaction energies of CO_2 with (a) benzene (C_6H_6) and (b) HBDC ($C_8H_6O_4$) as a function of intermolecular distances.

3. DEVELOPMENT OF FORCE FIELDS

3.1. High-Level Ab Initio Calculations and FF Fitting.

For notation, we use TZ, QZ, aTZ, and aQZ to denote cc-pVTZ, cc-pVQZ, aug-cc-pVTZ, and aug-cc-pVQZ bases, respectively. The use of diffuse functions is important to describe long-range correlation effects such as dispersion properly.[36] On the other hand, the choice of basis sets is also intimately tied to the choice of theoretical level of calculations, such as CCSD(T) versus MP2. While a rigorous approach would of course be to combine CCSD(T) with the high angular momentum basis augmented with diffuse functions, a practical limit of computational resources presently limits us to use RIMP2 for a large set of molecular complexes to train empirical FFs. Thus, as a pragmatic approach, we used the CCSD(T)/aTZ binding energy as a reference value, and performed the RIMP2 calculations with various basis sets (TZ, QZ, aTZ, and aQZ) to identify the basis set for RIMP2 that would give the closest CCSD(T)/aTZ binding energies (Table S2, Supporting Information (SI)). For prototypical CO_2−CO_2, benzene−CO_2, and $C_3N_3H_3$−CO_2 systems with various binding modes (eight conformations total), we observed that RIMP2/QZ yielded the smallest mean absolute deviation error relative to the CCSD(T)/aTZ calculations (Table S2). Therefore, RIMP2/QZ was used throughout all CO_2-MOF interaction calculations. Generally, adding diffuse functions increases binding energies in dispersion-dominated systems, but also MP2 is known to overestimate binding energies, and thus our numerical results that showed the closest binding energies for RIMP2/QZ relative to CCSD(T)/aTZ seem reasonable. For the CO_2−CO_2 interactions, however, since the system size is small enough, we used the reference CCSD(T)/aTZ calculations to derive the entire potential energy curves as a function of intermonomer distance.

The three parameters in the Morse potential function (D, α, and r_o in eq 1) were developed by fitting the QM results. We determined the 23 sets of interaction parameters for CO_2 uptake simulations of selected MOFs and ZIFs:

- CO_2−CO_2 interaction: C_{CO2}-C_{CO2}, O_{CO2}-O_{CO2}, C_{CO2}-O_{CO2}
- CO_2−MOF and ZIF interaction: C_R-C_{CO2}, C_R-O_{CO2}, O_R-C_{CO2}, O_R-O_{CO2}, N_R-C_{CO2}, N_R-O_{CO2}, Zn−C_{CO2}, Zn−O_{CO2}, H_-C_{CO2}, H_-O_{CO2}
- CO_2−functional group interaction: C_3-C_{CO2}, C_3-O_{CO2}, N_3-C_{CO2}, N_3-O_{CO2}, N_NO2-C_{CO2}, N_NO2-O_{CO2}, O_NO2-C_{CO2}, O_NO2-O_{CO2}, Cl_-C_{CO2}, Cl_-O_{CO2}

In these parameters, C_{CO2} and O_{CO2} denote the carbon and oxygen atoms in a CO_2 molecule, respectively. C_R, O_R, and N_R designate the aromatic carbon, oxygen, and nitrogen atoms in the frameworks, respectively; Zn denotes a zinc atom, and H_ designates a hydrogen atom bonded to the carbon and nitrogen. C_3 and N_3 designate the sp^3 carbon and nitrogen atoms in $-CH_3$ and $-NH_2$, respectively; N_NO2 and O_NO2 designate the nitrogen and oxygen atoms in the $-NO_2$ functional group; and Cl_ designates a chlorine atom in the -Cl functional group. The developed FFs are summarized in Table S3.

dx.doi.org/10.1021/jp307865n | J. Phys. Chem. C 2012, 116, 20254−20261

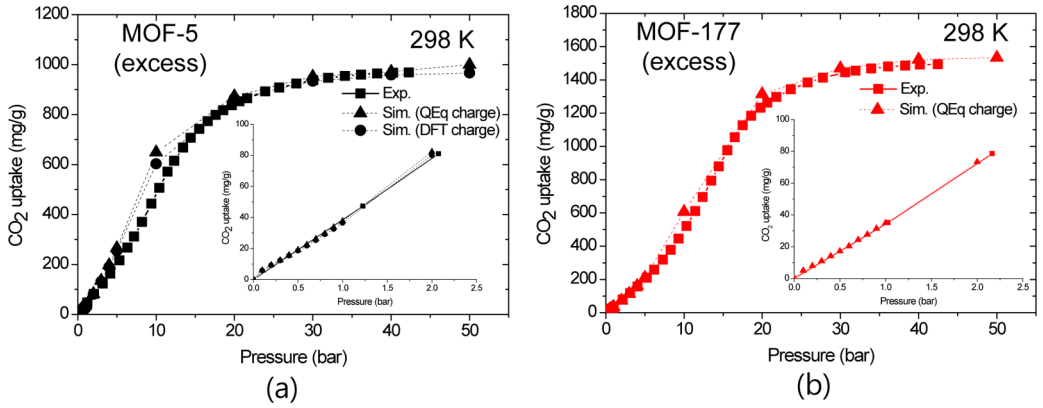

Figure 3. Excess CO_2 adsorption isotherms of (a) MOF-5 and (b) MOF-177 at 298 K. Symbol codes: triangle (Qeq), circle (DFT[8]), and square (experimental[38]). Here the error bars are smaller than the size of symbols.

To develop the CO_2−CO_2 interaction terms (C_{CO2}−C_{CO2}, O_{CO2}−O_{CO2}, and C_{CO2}−O_{CO2}), we considered a CO_2 dimer with two configurations (slipped parallel and T-shaped), which are shown in Figure 1a. Here, we used the atomic charges for carbon (+0.48222) and oxygen (−0.24111) atoms in the CO_2 molecule and a C═O bond length of 1.16042 Å, which were derived from the QM calculations. Our developed FFs reproduce reasonably well the QM-binding energies between two CO_2 molecules calculated at the CCSD(T)/aug-cc-pVTZ level, unlike the previous FFs[27] for the metal-decorated COF/CO_2 interactions where the curvatures calculated with the FFs were too steep compared to ab initio. In addition, we also computed the density of gas phase CO_2 at 273, 298, and 323 K by performing the GCMC simulations (Figure b) and observed a good agreement between our ab initio-based simulation results and the experiments.[37]

To develop the four interaction terms (C_R-C_{CO2}, C_R-O_{CO2}, H_-C_{CO2}, and H_-O_{CO2}) in CO_2−MOF (Figure 2a), we calculated the binding energies of CO_2 and benzene (C_6H_6) at the RI-MP2/cc-pVQZ level for three configurations: parallel, T-shaped (Vertical_1), and vertical to the edge (Vertical_2). Of the three configurations, the CO_2 parallel to the face of C_6H_6 has the highest binding energy (QM: −2.52 vs FF: −2.52 kcal/mol). The developed FF reproduces the QM potential energy surfaces notably well. To develop two interaction terms, such as O_R-C_{CO2} and O_R-O_{CO2} (Figure 2b), we calculated the CO_2 binding energies to HBDC with three configurations and found a good agreement between the QM and the developed FF. Indeed, for the configuration of CO_2 parallel to the face of HBDC, the QM binding energy is −2.78 kcal/mol, and the FF binding energy is −2.77 kcal/mol. Similarly, the N_R-C_{CO2} and N_R-O_{CO2} terms were determined by scanning the potential energy curves of CO_2 interacting with 1,3,5-triazine ($C_3N_3H_3$) (Figure S2).

For the FFs between functional groups (−CH_3, −NH_2, −NO_2, and −Cl) and CO_2, we used the benzene derivatives [$C_6H_3(CH_3)_3$, $C_6H_3(NH_2)_3$, $C_6H_3(NO_2)_3$, and $C_6H_3Cl_3$]. The comparisons between the QM and the developed FF are shown in Figure S3.

We note that the potential fits for the edge conformations have the largest discrepancies between the fitted and QM calculations. These large discrepancies between the fitted and QM calculations observed for the edge conformations can be explained by the use of fixed atomic charges in the FF fitting procedure in molecular complexes independent of the intermonomer distances. For example, for the $C_6H_3Cl_3/CO_2$ system that showed the largest error in the fitted binding energies for the edge conformation (Figure S3d), the fully relaxed QM charges for C and O of CO_2 modify significantly from 0.72 and −0.36 to 0.66 and −0.33, respectively, when the two separated $C_6H_3Cl_3$ and CO_2 monomers are brought together from 8 to 5.4 A. On the other hand, for the same system but with parallel configuration (Figure S3d), that shows an excellent agreement between the QM and fitted binding curves, the fully relaxed charges for C and O of CO_2 hardly change from 0.72 and −0.36 to 0.73 and −0.36, respectively, when the two separated monomers are brought to a distance 3.4 A.

3.2. FF Validation. To validate our new FFs, we performed the GCMC simulations for several known MOFs and ZIFs and compared the simulated CO_2 uptakes with the experimental[8,38,39] values. The structures and physical properties of the MOFs and ZIFs considered in this work are summarized in Figure S1 and in Table S1.

Figure 3 shows excess CO_2 adsorption isotherms of MOF-5 and MOF-177 at 298 K, where the atomic charges of the framework were assigned by the Qeq method, but in MOF-5, we also included an isotherm obtained with the DFT charges[38] for comparison. For the MOF-5, two different atomic charge schemes yield the similar CO_2 isotherm curves, also in good agreement with the reported experimental[29] data. Since the low-pressure CO_2 isotherm is very important for postcombustion CO_2 capture and separation, we included the magnified version of low-pressure CO_2 isotherms as insets.

Specifically, in Figure 3a, the MOF-5 isotherms at 298 K and 2 bar show an excellent agreement in CO_2 uptake between theory (82.2 mg/g) using new FFs and experiment (81.0 mg/g).[38] In an elevated pressure, i.e., 40 bar, the simulated and experimental uptakes also agree very well (971.5 and 967.0 mg/g, respectively). Similarly, for MOF-177 in Figure 3b, the simulated CO_2 isotherm agrees well with the reported experimental data[38] at both low and high pressure conditions. Since generally the CO_2 uptake at low pressures is mainly determined by the CO_2−MOF interactions, while the capacity at high pressure is determined by both the CO_2−MOF and CO_2−CO_2 interactions, the good agreements seen at both low and high pressures suggest that our FFs are accurate in describing both CO_2−MOF and CO_2−CO_2 interactions. Agreements between theory and experiments for ZIFs[8,39] are also tested and validated at low and high pressures. For

dx.doi.org/10.1021/jp307865n | J. Phys. Chem. C 2012, 116, 20254−20261

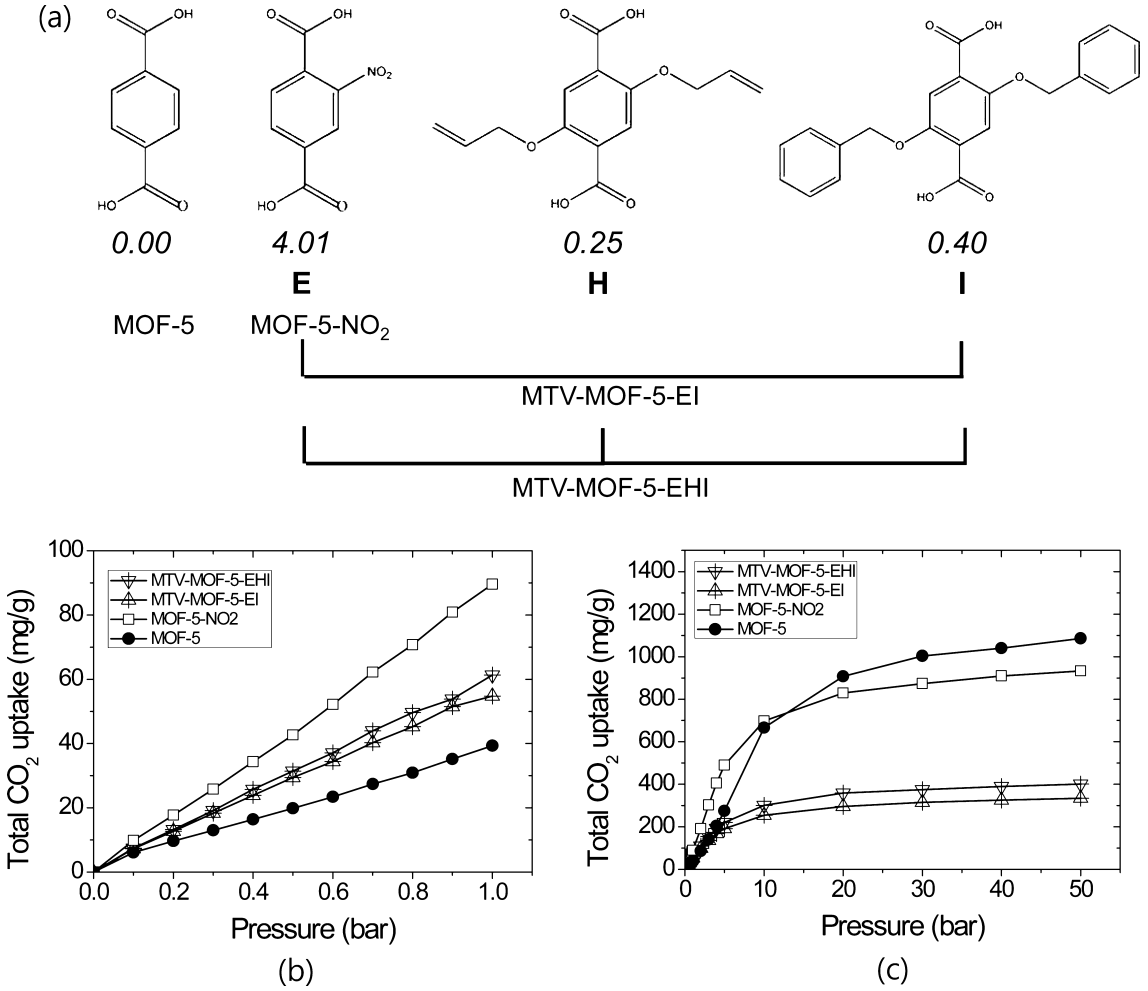

Figure 4. (a) MTV-MOFs (MTV-MOF-5-EI and MTV-MOF-5-EHI) structures where the numbers below organic linkers indicate their dipole moment in debye (D), and their total CO_2 adsorption isotherms at 298 K for (b) low and (c) high pressures.

example, for ZIF-8 (Figure S4a), the simulation and experiments[8] yield the CO_2 uptakes of 45.9 and 44.7 mg/g at 298 K and 1 bar, respectively, while for ZIF-68 (Figure S4b), the theoretical and experimental[39] uptakes are 73.7 and 71.2 mg/g, respectively, under the same conditions.

Despite good agreements between simulation and experiments at low and high pressures, in Figure 3, our GCMC simulations overestimate uptake values for moderate pressure ranges (5−15 bar) where the rapid increase in CO_2 uptake (inflection behavior) begins to occur in the S-shaped isotherms. It has been suggested[38] that the CO_2 uptake amounts near these inflection pressures are *very sensitive* to the atomic charges of CO_2 since the attractive electrostatic interactions between CO_2 molecules become very important at these moderate pressures (5−15 bar) and room temperature. We then took a step further in this study and additionally considered the effects of framework charges, not just CO_2 charges, by comparing the simulated CO_2 uptakes with Qeq (fast but less accurate) and DFT (slow but more accurate) charges. In Figure 3a, we find that the use of more accurate DFT charges indeed improve the simulation result to agree better with experiments for pressure ranges 5−15 bar. This result, together with the previous indication[38] for the importance of CO_2 charges in the latter pressure regions, suggests that both framework and CO_2 charges are important for theoretical prediction of CO_2 uptakes at moderate pressures (5−15 bar), and in this context, the charges used in our GCMC simulations may have room for further improvements to reproduce the experimental results better in these very sensitive regions. Of course, the CO_2 uptake at the moderate pressures is also affected by the vdW interactions.

4. APPLICATIONS

4.1. MTV-MOFs and Local Dipole Moments. On the basis of the MOF-5 type structure, Deng et al.[40] recently synthesized 18 MTV-MOFs that contain up to eight distinct functionalities in one phase, and showed that the MTV-MOFs can take up a larger amount of CO_2 gas than does the pristine MOF-5. In this work, we explain the origin of the enhanced CO_2 uptake in the MTV-MOFs by using accurate QM-based FFs

We considered two MTV-MOFs, MTV-MOF-5-EI and MTV-MOF-5-EHI, as in the experiment,[40] where the former has the $-NO_2$ (denoted by "E") and $-(OC_7H_5)_2$ (I) functional groups, and the latter has the $-NO_2$ (E), $-(OC_3H_5)_2$ (H), and $-(OC_7H_5)_2$ (I) functional groups (Figure 4a). Figure 4b and 4c show the simulated total CO_2 adsorption isotherms of the MTV-MOFs at 298 K, with MOF-5 and MOF-5-NO_2 also included for comparison. At 1 bar (Figure 4b), both MTV-MOFs show a higher CO_2 uptake amount than does the pristine MOF-5, in good agreement with experiments;[40] however, surprisingly, the CO_2 uptake amount of MOF-5-

dx.doi.org/10.1021/jp307865n | J. Phys. Chem. C 2012, 116, 20254−20261

NO_2 (not yet reported experimentally) at 1 bar is predicted to be larger than those of EI and EHI MTV-MOFs. Interestingly, but perhaps as expected, at 50 bar (Figure 4c), the CO_2 uptake shows the trend that follows the pore volumes: MOF-5 (1085.5 mg/g) > MOF-5-NO_2 (933.2 mg/g) > MTV-MOF-5-EHI (400.9 mg/g) > MTV-MOF-5-EI (334.4 mg/g) versus MOF-5 (1.30 cm^3/g) > MOF-5-NO_2 (1.01 cm^3/g) > MTV-MOF-5-EHI (0.65 cm^3/g) > MTV-MOF-5-EI (0.56 cm^3/g).

In modeling structures of the MTV-MOFs, the ratio of functionalities was taken from the experimental[40] data. In other words, for MTV-MOF-5-EI, the ratio of links E and I is E:I = 1:1, and for MTV-MOF-5-EHI, E:H:I = 1:1:1. The functionalities were then randomly distributed in MOF-5 structures. Of course, the CO_2 uptake of MTV-MOFs would depend on the arrangement and ratio of the functionalities, and details of the latter aspects will be reported in the next paper.

To understand our prediction that MOF-5-NO_2 shows a higher CO_2 uptake amount than do other experimental MTV-MOFs at low pressures, we again calculated the dipole moments of the organic linkers E, H, and I. The organic linkers E, H, and I have dipole moments of 4.01, 0.25, and 0.40 D, respectively, implying that the MOF just composed of the organic linker E (MOF-5-NO_2) would be more polarized than those involving H or/and I. Due to its significant quadrupolar moment, the CO_2 binding is sensitive to the framework polarity,[41] and for that reason, MOF-5-NO_2 is expected to have a more favorable electrostatic interaction with CO_2 compared to other MTV-MOFs.

To support our prediction and arguments further, we considered the relative contribution of the framework-gas electrostatic interactions to the total CO_2 uptake and simulated the CO_2 adsorption isotherms by turning off the CO_2-MOF electrostatic interactions while just maintaining the CO_2–CO_2 electrostatic interactions. The vdW terms were always included in both sets of simulations. As shown in Figure 5, the CO_2-MOF electrostatic contribution to the total CO_2 uptake at 298 K and 1 bar is approximately 25% in the MTV-MOFs, much greater than 10% in the pristine MOF-5. Moreover, the MTV-MOFs have a smaller pore volume than MOF-5 by introducing the protruding functional groups, which usually means a tighter or stronger vdW interaction between the framework and gas molecules. Therefore, it appears that both electrostatic (due to increased dipole moments) and vdW (due to tighter geometry) interactions in the MTV-MOFs contribute favorably to the increased CO_2 uptake amount. More interestingly, MOF-5-NO_2 has an even higher electrostatic contribution (35%) to the total uptake as compared to the latter MTV-MOFs, consistent with the calculated dipole moments of the corresponding organic linkers. Accordingly, the enhanced electrostatic interaction in MOF-5-NO_2 seems to be the key to the higher CO_2 uptake found in our predictions as compared to the MTV-MOFs. Of course, the lower weight per unit cell of MOF-5-NO_2 than that of MTV-MOFs also contributes to the greater CO_2 uptake in milligrams per gram (mg/g) units. In addition, both of the MTV-MOF-EI and -EHI have bulky functionalities (H and I) and dipole moments of the functionalities H and I are much lower than the E, which leads to the larger contribution of the vdW interaction than that of the electrostatic interaction. Thus, the deviation for the two MTV-MOFs is not large.

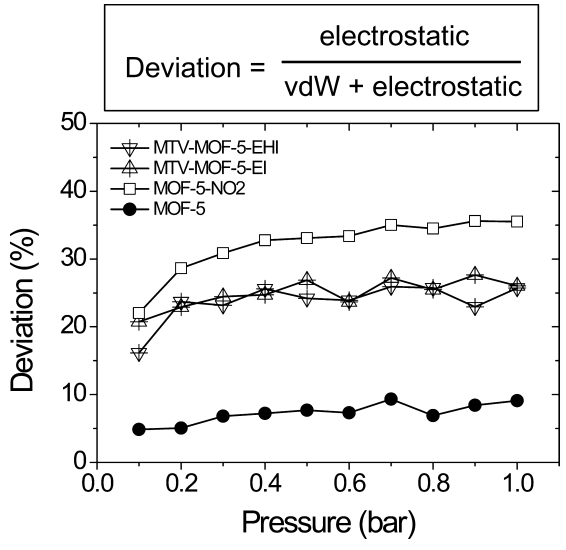

Figure 5. Relative contribution of the MOF-CO_2 electrostatic interactions to the total uptake by calculating the deviation of the adsorbed CO_2 amount between with and without including the electrostatic interactions in MOF-5, MOF-5-NO_2, MTV-MOF-5-EI, and MTV-MOF-5-EHI as a function of pressure.

4.2. Introducing Both Electron-Donating and -Withdrawing Groups Simultaneously in the Organic Linker.

In recent years, several experimental and theoretical studies have reported that CO_2 uptake can be improved by incorporating proper functional groups into the framework.[20,41−46] These studies suggested that the dipole moment of an organic linker could be considered as one of the criteria for CO_2 adsorption enhancement,[41] and that the asymmetric functionalization of the organic linker can also lead to a high CO_2 uptake.[20] Now equipped with accurate FFs for several MOF functional groups (e.g., $-CH_3$, $-NH_2$, $-Cl$, $-NO_2$, $-C_4H_4$, and $-OC_3H_5$) interacting with CO_2, we investigated the effects of introducing electron-donating and -withdrawing groups, denoted as EDG and EWG, respectively, into the organic linker. In particular, we studied the additive or nonadditive effects by combining EDG and EWG together into the same organic linker.

Using MOF-5 as a base structure, we considered three functionalizations of different electronic nature, MOF-5-NO_2 (EWG), MOF-5-NO_2–NH_2 (EWG+EDG), and MOF-5-NO_2–Cl (EWG+EWG). Cartoons of these structures and the simulated CO_2 adsorption isotherms for these MOFs at 298 K up to 1 bar are shown in Figure 6. All functional groups considered here clearly improve the CO_2 uptake. For example, at 298 K and 1 bar, MOF-5 shows a total CO_2 uptake of 39.3 mg/g, while MOF-5-NO_2 shows a total CO_2 uptake of 89.6 mg/g. Interestingly, we find that such an enhancement is even more pronounced by a combination of both EDG and EWG, whereas a combination of two EWGs actually lowers the CO_2 uptake even than when just one EWG is used. At 298 K and 1 bar, MOF-5-NO_2-NH_2 shows a total CO_2 uptake of 94.3 mg/g, which is higher than 89.6 mg/g of MOF-5-NO_2 or 77.3 mg/g of MOF-5-NO_2-Cl. Intriguingly, we find that the latter capacity trend of various MOFs is indeed consistent with the order of dipole moments of organic linker, MOF-5-NO_2-NH_2 (7.39 D) > MOF-5-NO_2 (4.01 D) > MOF-5-NO_2-Cl (3.44 D) > MOF-5 (0.00 D), indicating the importance of dipole moment of the linker and its electronic interactions with quadrupole moment of CO_2.[41] Indeed, the contribution of MOF-CO_2 electrostatic interaction to CO_2 uptake follows the order of the dipole

dx.doi.org/10.1021/jp307865n | J. Phys. Chem. C 2012, 116, 20254−20261

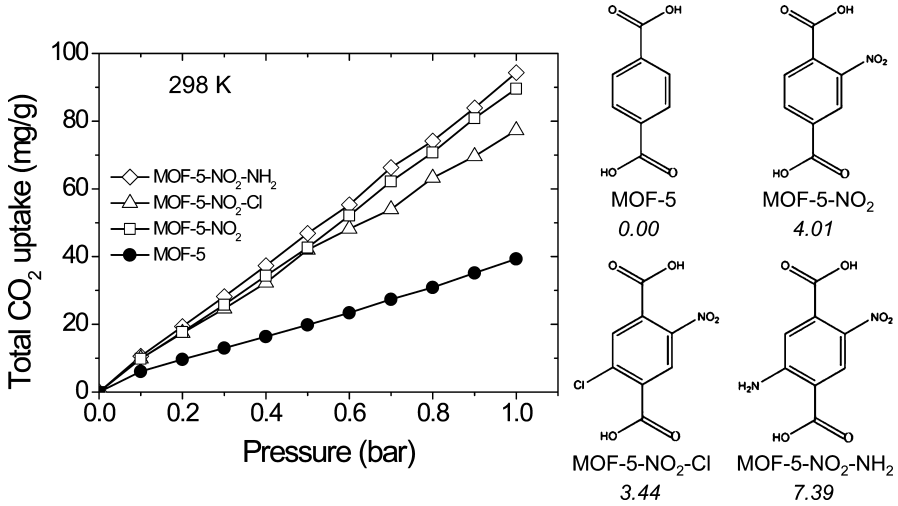

Figure 6. Effects of functional groups on the CO_2 uptake of MOFs, where the numbers below organic linkers indicate their dipole moment in debye (D).

moment: MOF-5-NO_2-NH_2 > MOF-5-NO_2 > MOF-5-NO_2-Cl > MOF-5. Here, initial heat of adsorption (Q_{st}) of CO_2 is 4.7 kcal/mol for MOF-5-NO_2−NH_2, 4.4 kcal/mol for MOF-5-NO_2, 4.5 kcal/mol for MOF-5-NO_2-Cl, and 3.2 kcal/mol for MOF-5. For a comparison, MTV-MOF-5-EI and -EHI have 5.3 and 5.0 kcal/mol, respectively.

5. CONCLUSIONS

The MOFs and ZIFs are regarded as promising candidates for CO_2 capture. Currently, numerous MOF-type materials have been reported, which indicates an urgent need for a rapid technique for reliable screening and design of the new structures with desirable properties. In this study, we developed ab initio derived FFs for accurately simulating the CO_2 uptake in various MOFs and ZIFs. Transferability of the conventional FFs is generally of concern when used for known systems. If the FFs were developed from experimental data for specific MOFs/ZIFs, their transferability would indeed be a concern. However, since our "atomic" FFs are developed based on the ab initio calculations of CO_2 binding to the separate components of MOFs/ZIFs (metal oxide part, organic linker part, and functional groups), and not from specific data on specific systems, the transferability of our FFs would not be of as major concern as in conventional FFs that were fitted against experimental data of specific systems. In fact, the independent tests of our FFs to the several known experimental systems (that were not used in our FF fitting procedure) and the good agreement found there indeed suggest that our FFs should have a better transferability than the conventional FFs fitted using specific experimental data.

Through GCMC simulations with accurate FFs, we can now quickly and reliably predict CO_2 adsorption isotherms up to a high pressure, e.g., 50 bar, and guide experiments. For example, our simulated electronic substituent effects suggest introducing both electron-donating and -withdrawing functional groups simultaneously in the same organic linker can increase the CO_2 capacity noticeably at low pressure through more favorable electrostatic interactions with CO_2. Using these new FFs, we also found that the underlying mechanism of the enhanced CO_2 uptake in recently synthesized MTV-MOFs is a combination of both increased dipole moments of the linker (electrostatic) and tighter geometry given by a smaller pore volume (vdW) in the MTV-MOFs. To this end, we predict that MOF-5-NO_2 can have a even higher CO_2 uptake than the existing MTV-MOFs due to a larger local dipole moment (electrostatic interactions).

■ ASSOCIATED CONTENT

Ⓢ Supporting Information

Structures and physical properties of MOFs and ZIFs investigated in this study, models and computational details, detailed procedure of the FF development and validation along with the summary of optimized parameters, and the tabulated CO_2 uptake amounts in MOFs and ZIFs reported in this work. This material is available free of charge via the Internet at http://pubs.acs.org.

■ AUTHOR INFORMATION

Corresponding Author

*E-mail: sangsoo@kriss.re.kr (S.S.H.); ysjn@kaist.ac.kr (Y.J.).

Notes

The authors declare no competing financial interest.

■ ACKNOWLEDGMENTS

We thank Prof. Omar M. Yaghi and Dr. Hiroyasu Furukawa for helpful comments. This research was performed for the Hydrogen Energy R&D Center, of the 21st Century Frontier R&D program, funded by the Ministry of Education, Science and Technology (MEST) of Korea. Y.J. acknowledges the support from WCU program (R31-2008-000-10055-0) and Korea CCS R&D Center funded by MEST. The modeling software was kindly provided by Accelrys Korea.

■ REFERENCES

(1) Furukawa, H.; Ko, N.; Go, Y. B.; Aratani, N.; Choi, S. B.; Choi, E.; Yazaydin, A. Ö.; Snurr, R. Q.; O'Keeffe, M.; Kim, J.; Yaghi, O. M. *Science* **2010**, *329*, 424.

(2) Farha, O. K.; Yazaydin, A. Ö.; Eryazici, I.; Malliakas, C. D.; Hauser, B. G.; Kanatzidis, M. G.; Nguyen, S. T.; Snurr, R. Q.; Hupp, J. T. *Nat. Chem.* **2010**, *2*, 944.

(3) Park, K. S.; Ni, Z.; Côté, A. P.; Choi, J. Y.; Huang, R.; Uribe-Romo, F. J.; Chae, H. K.; O'Keeffe, M.; Yaghi, O. M. *Proc. Natl. Acad. Sci. U.S.A.* **2006**, *103*, 10186.

(4) Phan, A.; Doonan, C. J.; Uribe-Romo, F. J.; Knobler, C. B.; O'Keeffe, M.; Yaghi, O. M. *Acc. Chem. Res.* **2010**, *43*, 58.

(5) Sumida, K.; Rogow, D. L.; Mason, J. A.; McDonald, T. M.; Bloch, E. D.; Herm, Z. R.; Bae, T.-H.; Long, J. R. *Chem. Rev.* **2012**, *112*, 724.
(6) Bae, Y.-S.; Snurr, R. Q. *Angew. Chem., Int. Ed.* **2011**, *50*, 11586.
(7) Xiang, Z.; Cao, D.; Lan, J.; Wang, W.; Broom, D. P. *Energy Environ. Sci.* **2010**, *3*, 1469.
(8) Yazaydin, A. Ö.; Snurr, R. Q.; Park, T.-H.; Koh, K.; Liu, J.; LeVan, M. D.; Benin, A. I.; Jakubczak, P.; Lanuza, M.; Galloway, D. B.; Low, J. J.; Willis, R. R. *J. Am. Chem. Soc.* **2009**, *131*, 18198.
(9) Babarao, R.; Jiang, J. *Langmuir* **2008**, *24*, 6270.
(10) Rankin, R. B.; Liu, J.; Kulkarni, A. D.; Johnson, J. K. *J. Phys. Chem. C* **2009**, *113*, 16906.
(11) Sirjoosingh, A.; Alavi, S.; Woo, T. K. *J. Phys. Chem. C* **2010**, *114*, 2171.
(12) Liu, B.; Smit, B. *J. Phys. Chem. C* **2010**, *114*, 8515.
(13) McDaniel, J. G.; Yu, K.; Schmidt, J. R. *J. Phys. Chem. C* **2012**, *116*, 1892.
(14) Zheng, C.; Liu, D.; Yang, Q.; Zhong, C.; Mi, J. *Ind. Eng. Chem. Res.* **2009**, *48*, 10479.
(15) Wilmer, C. E.; Snurr, R. Q. *Chem. Eng. J.* **2011**, *171*, 775.
(16) Rappé, A. K.; Goddard, W. A., III. *J. Phys. Chem.* **1991**, *95*, 3358.
(17) Haldoupis, E.; Nair, S.; Sholl, D. S. *J. Am. Chem. Soc.* **2012**, *134*, 4313.
(18) Rappé, A. K.; Casewit, C. J.; Colwell, K. S.; Goddard, W. A., III; Skiff, W. M. *J. Am. Chem. Soc.* **1992**, *114*, 10024.
(19) Mayo, S.; Olafson, B.; Goddard, W. A., III. *J. Phys. Chem.* **1990**, *94*, 8897.
(20) Morris, W.; Leung, B.; Furukawa, H.; Yaghi, O. K.; He, N.; Hayashi, H.; Houndonougbo, Y.; Asta, M.; Laird, B. B.; Yaghi, O. M. *J. Am. Chem. Soc.* **2010**, *132*, 11006.
(21) Bae, Y.-S.; Mulfort, K. L.; Frost, H.; Ryan, P.; Punnathanam, S.; Broadbelt, L. J.; Hupp, J. T.; Snurr, R. Q. *Langmuir* **2008**, *24*, 8592.
(22) Rankin, R. B.; Liu, J.; Kulkarni, A. D.; Johnson, J. K. *J. Phys. Chem. C* **2009**, *113*, 16906.
(23) Han, S. S.; Deng, W. Q.; Goddard, W. A., III. *Angew. Chem., Int. Ed.* **2007**, *46*, 6289.
(24) Han, S. S.; Furukawa, H.; Yaghi, O. M.; Goddard, W. A., III. *J. Am. Chem. Soc.* **2008**, *130*, 11580.
(25) Han, S. S.; Choi, S.-H.; Goddard, W. A., III. *J. Phys. Chem. C* **2010**, *114*, 12039.
(26) Mendoza-Cortés, J. L.; Han, S. S.; Furukawa, H.; Yaghi, O. M.; Goddard, W. A., III. *J. Phys. Chem. A* **2010**, *114*, 10824.
(27) Lan, J.; Cao, D.; Wang, W.; Smit, B. *ACS Nano* **2010**, *4*, 4225.
(28) Raghavachari, K.; Trucks, G. W.; Pople, J. A.; Head-Gordon, M. *Chem. Phys. Lett.* **1989**, *157*, 479.
(29) (a) Møller, C.; Plesset, M. S. *Phys. Rev.* **1934**, *46*, 618. (b) Weigend, F.; Häser, M. *Theor. Chem. Acc.* **1997**, *97*, 331. (c) Ahlrichs, R.; Bär, M.; Häser, M.; Horn, H.; Kölmel, C. *Chem. Phys. Lett.* **1989**, *162*, 165.
(30) *Q-CHEM Software*, version 4.0; Q-Chem Inc.: Pittsburgh, PA, 2011.
(31) (a) Illies, A. J.; McKee, M. L.; Schlegel, H. B. *J. Phys. Chem.* **1987**, *91*, 3489. (b) Welker, M.; Steinebrunner, G.; Solca, J.; Huber, H. *Chem. Phys.* **1996**, *213*, 253. (c) Bock, S.; Bich, E.; Vogel, E. *Chem. Phys.* **2000**, *257*, 147.
(32) Dunning, T. H., Jr. *J. Chem. Phys.* **1989**, *90*, 1007.
(33) Simons, S.; Duran, M.; Dannenberg, J. J. *J. Chem. Phys.* **1996**, *105*, 11024.
(34) Zhou, W.; Wu, H.; Hartman, M. R.; Yildirim, T. *J. Phys. Chem. C* **2007**, *111*, 16131.
(35) *The Cerius2 Software*, version 4.10; Accelrys, Inc.: San Diego, CA, 2009.
(36) Vogiatzis, K. D.; Mavrandonakis, A.; Klopper, W.; Froudakis, G. E. *ChemPhysChem* **2009**, *10*, 374.
(37) Thermophysical Properties of Fluid Systems; *NIST Standard Reference Database*; National Institute of Standards and Technology: Gaithersburg, MD, 2005.
(38) Walton, K. S.; Millward, A. R.; Dubbeldam, D.; Frost, H.; Low, J. J.; Yaghi, O. M.; Snurr, R. Q. *J. Am. Chem. Soc.* **2008**, *130*, 406.
(39) Benerjee, R.; Furukawa, H.; Britt, D.; Knobler, C.; O'Keeffe, M.; Yaghi, O. M. *J. Am. Chem. Soc.* **2009**, *131*, 3875.
(40) Deng, H.; Doonan, C. J.; Furukawa, H.; Ferreira, R. B.; Towne, J.; Knobler, C. B.; Wang, B.; Yaghi, O. M. *Science* **2010**, *327*, 846.
(41) Amrouche, H.; Aguado, S.; Pérez-Pellitero, J.; Chizallet, C.; Siperstein, F.; Farrusseng, D.; Bats, N.; Nieto-Draghi, C. *J. Phys. Chem. C* **2011**, *115*, 16425.
(42) Chen, Z.; Xiang, S.; Arman, H. D.; Li, P.; Tidrow, S.; Zhao, D.; Chen, B. *Eur. J. Inorg. Chem.* **2010**, 3745.
(43) Chen, Z.; Xiang, S.; Arman, H. D.; Li, P.; Zhao, D.; Chen, B. *Eur. J. Inorg. Chem.* **2011**, 2227.
(44) Chen, Z.; Xiang, S.; Arman, H. D.; Mondal, J. U.; Li, P.; Zhao, D.; Chen, B. *Inorg. Chem.* **2011**, *50*, 3442.
(45) Xiang, S.; He, Y.; Zhang, Z.; Wu, H.; Zhou, W.; Krishna, R.; Chen, B. *Nat. Chem.* **2012**, *3*, 954.
(46) (a) Park, J.; Kim, H.; Han, S. S.; Jung, Y. *J. Phys. Chem. Lett.* **2012**, *3*, 826. (b) Park, J. Y.; Lee, Y. S.; Jung, Y. *J. Nanoparticle Res.* **2012**, *14*, 793. (c) Patel, H. A.; Karadas, F.; Canlier, A.; Park, J.; Deniz, E.; Jung, Y.; Atilhan, M.; Yavuz, C. T. *J. Mater. Chem.* **2002**, *22*, 8431. (d) Zulflgar, S.; Karadas, F.; Park, J.; Stucky, G. D.; Jung, Y.; Atilhan, M.; Yavuz, C. T. *Energy Environ. Sci.* **2011**, *4*, 4528.